Crystallisation of Amorphous $Y_{50}Cu_{42}Al_8$ Alloy

B. Idzikowski, Z. Śniadecki and B. Mielniczuk

Institute of Molecular Physics, Polish Academy of Sciences

M. Smoluchowskiego 17, 60-179 Poznań, Poland

Amorphous $Y_{50}Cu_{42}Al_8$ ribbon was prepared by melt-spinning technique on the Cu wheel. The crystallisation process was analysed by differential scanning calorimetry and X-ray diffraction. Differential scanning calorimetry curves characterising two crystallisation stages of $Y_{50}Cu_{42}Al_8$ alloy were measured in non-isothermal dynamic mode at different heating rates. Activation energies of both steps of crystallisation process were acquired by the Kissinger method and are equal to 570 ± 56 and 290 ± 29 kJ/mol for the first and second stage, respectively. By annealing the ribbon at a given temperature for various times the nanocrystalline phase grains of the sizes of about 40 nm in diameter were created. The influence of the annealing temperature on the grain size evolution was also examined.

PACS numbers: 61.43.Dq, 61.82.Bg, 81.07.Bc, 81.70.Pg

1. Introduction

Alloys of the amorphous/nanocrystalline composite structure have been a subject of considerable interest for the last few years mainly because of their unique physical properties in comparison with those of their fully crystalline and amorphous counterparts. Crystallisation of amorphous alloys caused e.g. by heat treatment leads to evolution of the nanocrystalline structure that changes its initial properties. The properties of the nanocrystalline compounds depend mainly on their structure and phase attributes like crystalline volume fraction and mean grain size.

The main aim of the study reported in this paper was to determine the structure, chemical composition and nanocrystals growth kinetics in amorphous $Y_{50}Cu_{42}Al_8$ by examination of the crystallisation process. This alloy belongs to $Y_xCe_{50-x}Cu_{42}Al_8$ series and in our further investigation it will be used as the non-magnetic analogue of other Ce-containing samples. We intend to observe the influence of partial substitution of Y by Ce on the magnetic, possibly heavy-fermion properties and structural changes in the amorphous and nanocrystalline alloys of different crystalline grain sizes. The unique properties of Ce such as the variable electronic structure and unstable valence states are preconditions of strongly correlated electron phenomena [1] which have been also found in some amorphous or nanocrystalline Ce-based metallic alloys [2, 3]. The composition of the alloys to be studied has been chosen also because of their significant glass forming ability necessary to prepare fully amorphous ribbon [4] for controlled crystallisation by heat treatment.

2. Experimental

The $Y_{50}Cu_{42}Al_8$ ingot has been prepared by arc--melting under the protective atmosphere of argon. It has been subsequently rapidly quenched in a melt-spinning device on the copper wheel of the surface velocity of 40 m/s. The obtained ribbons were 20 μm thick and 1.2 mm wide. The thermal behaviour of the alloy was studied by differential scanning calorimetry (DSC) measurements using the Netzsch DSC 404 apparatus at the heating rates q from 10 to 40 K/min and in the temperature range T from 50 to 900°C under a continuous argon flow at a constant rate. Crystallisation of amorphous alloys was induced by isothermal heat treatment for different times and temperatures determined from DSC curves. The crystalline structure of as-quenched and annealed ribbons was examined by the X-ray diffraction with Co K_α radiation in the Bragg–Brentano geometry.

3. Results and discussion

The DSC traces of melt-spun $Y_{50}Cu_{42}Al_8$ with $q = 10$ and 40 K/min are shown in Fig. 1. Two exothermic crystallisation peaks have been observed. The first crystallisation stage has the onset temperatures T_{o1} from 284.1 to 290.0°C and the peak temperatures T_{x1} from 287.0 to 293.0°C for the heating rates q from 10 to 40 K/min, respectively. The second peak temperatures T_{x2} are from 373.8 to 389.5°C for the same range of heating rates. The onset temperatures T_{o2} of the second peak have not been well determined because of broad peak shape.

The glass transition effect has not been observed on the DSC curves. The temperature T_g characteristic of this effect may be close to the crystallisation onset temperature in this system or it cannot be observed using the standard constant-heating DSC scans, as e.g. for some Al-based metallic glasses [5]. The presence of dispersed polyamorphous packings with a wide range of local glass transitions is also possible [6].

The enthalpy ΔH of the two processes corresponding to the DSC peaks was determined using the software dedicated for the Netzsch DSC 404 apparatus. It did not

change significantly with q and was $\Delta H = 34.6$ for the first peak and $\Delta H = 1.3$ J/g for the second peak, respectively.
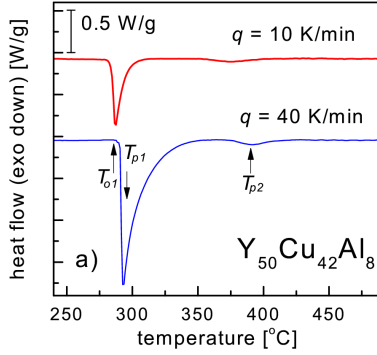

Fig. 1. Heat flow as a function of temperature, examined at a constant heating rate q of 10 and 40 K/min.
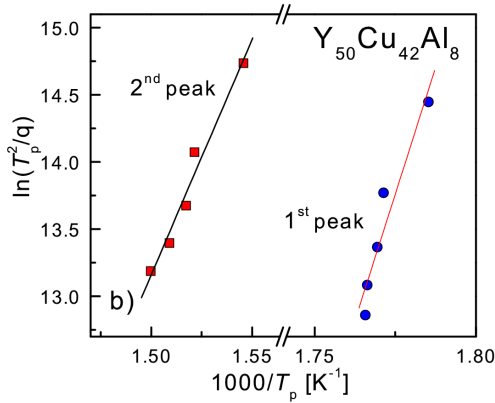

Fig. 2. Kissinger plot for both crystallisation events for melt-spun $Y_{50}Cu_{42}Al_8$ ribbon (b).

The activation energies of crystallisation E_a of the alloy studied were calculated using the Kissinger analysis [7] on the basis of the plots shown in Fig. 2. The E_a values are $E_a = 569 \pm 56$ kJ/mol for the first peak and $E_a = 292 \pm 29$ kJ/mol for the second one.

The X-ray diffraction (XRD) method was applied in order to confirm the amorphous state of the as-quenched ribbons and to identify the products of the crystallisation and also to determine its parameters. The XRD patterns in Fig. 3 show the evolution of the structure of $Y_{50}Cu_{42}Al_8$ caused by heat treatment at $T_a = 270°C$ (close to the crystallisation onset temperature T_{o1}) for τ from 15 to 60 min, and additionally at $T_a = 450°C$ for $\tau = 15$ min.

The as-quenched alloy was found to be in the uniform amorphous phase with no long-range atomic ordering detected by XRD. The annealed ribbons contain the crystalline phases and the residual amorphous one. There are two main crystalline constituents growing du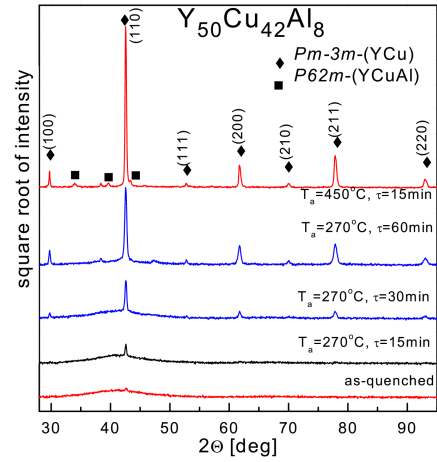ring isothermal annealing at $T_a = 270°C$. The first appearing phase is YCu with the ClCs-type structure (Pm-$3m$ space group) embedded in an amorphous matrix. The second one is YCuAl and it forms on annealing at this temperature for over 30 min and/or by annealing at temperatures above the first crystallisation peak. According to Shi et al. [8] the lattice constant of the YCu phase is $a = 3.476$ Å and the cell volume $v_c = 41.999$ Å^3. The analogous values determined on the basis of XRD patterns are $a = 3.490$ Å and $v_c = 42.509$ Å^3. The YCuAl phase is Fe$_2$P-type ($P62m$ space group) and its lattice parameters are $a = 7.022$ Å, $c = 4.033$ Å and lattice volume $v_c = 17.220$ Å^3 [9]. Experimentally determined values for YCuAl are $a = 7.025$ Å, $c = 3.996$ Å, $v_c = 17.221$ Å^3. The diffraction peaks are slightly shifted by the same angle value in comparison with the diffraction patterns based on lattice parameters obtained by Krachan et al. [9]. The change can be caused by the lattice cell distortion because of the influence of amorphous matrix and coexisting phases with some randomness in Cu by Al atoms substitution [9].

The sample was also annealed at 450°C for 15 min to examine the structural composition of the fully crystallised alloy. After annealing, the main phase was YCu (over 92%) with a small amount of YCuAl (about 7%) and Y_2O_3 oxides (below 1%).

The volume fraction X, defined as $X = A_{cr}/(A_{cr} + A_{am})$ [10], where A_{cr} is the YCu phase (110) peak area and A_{am} corresponds to the area of amorphous $halo$ of the YCu phase was obtained from the X-ray diffraction patterns shown in Fig. 3. On annealing the alloy at $T_a = 270°C$ for different times τ, the volume fraction of crystalline phase changed from 13.8% for $\tau = 15$ min to 91.9% for $\tau = 60$ min.

The average grain size D (mean diameter) of the YCu phase was determined from the main peak (110) of the XRD patterns according to the Scherrer formula. The dependences of the mean grain size on the time of annealing τ and on the temperature of annealing T_a are

Fig. 3. XRD patterns of as-quenched and annealed $Y_{50}Cu_{42}Al_8$ alloys.

shown in Fig. 4. The D value for this alloy annealed at $T_a = 270°$C for different τ decreased slightly with increasing time of annealing and it is of about 40 nm for τ from 15 to 60 min range (Fig. 4a). The absence of grain growth process with increasing crystalline volume fraction means that the crystallisation proceeds mainly by the formation of new nucleation centres rather than by the growth of grains.
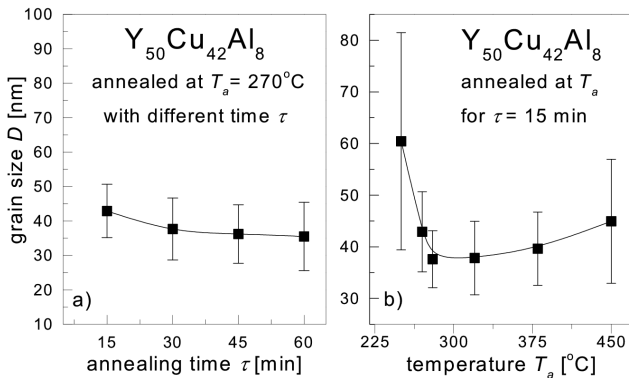

Fig. 4. Grain size of Y$_{50}$Cu$_{42}$Al$_8$ annealed at different times (a) and temperatures (b).

The grain size was also determined for different annealing temperatures T_a with constant annealing time $\tau = 15$ min (Fig. 4b). With T_a increasing from 250°C to 280°C the mean grain size value decreases with its minimum around $T_a = 280°$C and then it increases up to the complete crystallisation of the sample. This behaviour has been already observed for different systems (i.e. Fe–Si–B [11] or Fe–B [12]) and it is caused by variations in the crystal growth rate and nucleation rate with annealing temperature. The growth of primary crystals may be also dependent on their morphology [11, 12].

4. Summary

The crystallisation behaviour of as-quenched, fully amorphous Y$_{50}$Cu$_{42}$Al$_8$ ribbon is governed by two exothermic reactions. There are two main phases appearing during annealing of the as-quenched alloy: YCu and YCuAl. Upon the heat treatment at a temperature close to the crystallisation onset the crystalline volume fraction X increases with the time of annealing τ but the mean grain size D does not change significantly. It suggests that during the crystallisation process the forma-

tion of new nucleation centres dominates over the growth of grains. It can be concluded that it is possible to obtain a nanocrystalline structure of desired grain size by controlling the size of the crystallisation products at appropriate annealing conditions.

The obtained structural and crystallisation parameters (effective activation energies and crystallisation enthalpies) will be the reference for further investigation of Y$_x$Ce$_{50-x}$Cu$_{42}$Al$_8$ system with different Y substitution by Ce. The structural changes and heavy-fermion properties of Y$_x$Ce$_{50-x}$Cu$_{42}$Al$_8$ series will be the subject of further investigation based on the results described above.

5. Acknowledgments

References

[1] E. Bauer, *Adv. Phys.* **40**, 417 (1991).

[2] S.-W. Han, C.H. Booth, E.D. Bauer, P.H. Huang, Y.Y. Chen, J.M. Lawrence, *Phys. Rev. Lett.* **97**, 097204 (2006).

[3] Y.Y. Chen, Y.D. Yao, C.R. Wang, W.H. Li, C.L. Chang, T.K. Lee, T.M. Hong, J.C. Ho, S.F. Pan, *Phys. Rev. Lett.* **84**, 4990 (2000).

[4] B. Zhang, R.J. Wang, D.Q. Zhao, M.X. Pan, W.H. Wang, *Phys. Rev. B* **70**, 224208 (2004).

[5] P. Kerschl, U.K. Rössler, T. Gemming, K.-H. Müller, Z. Śniadecki, B. Idzikowski, *Appl. Phys. Lett.* **90**, 31903 (2007).

[6] H.W. Sheng, H.Z. Liu, Y.Q. Cheng, J. Wen, P.L. Lee, W.K. Luo, S.D. Shastri, E. Ma, *Nature Mater.* **6**, 192 (2007).

[7] H.E. Kissinger, *Anal. Chem.* **29**, 1702 (1957).

[8] Y.J. Shi, Y.L. Du, G. Chen, G.L. Chen, *Phys. Lett. A* **368**, 495 (2007).

[9] T. Krachan, B. Stelmakhovych, Yu. Kuzma, *J. Alloys Comp.* **349**, 134 (2003).

[10] T. Gloriant, M. Gich, S. Surinach, M.D. Baro, A.L. Greer, *J. Metastable Nanocryst. Mater.* **8**, 365 (2000).

[11] H.Y. Tong, B.Z. Ding, H.G. Jiang, K. Lu, J.T. Wang, Z.Q. Hu, *J. Appl. Phys.* **75**, 654 (1994).

[12] A.L. Greer, *Acta Metall.* **30**, 171 (1982).